

Isolation and Phase Space Energization Analysis of the Corrugation Instability with the Field-Particle Correlation Technique

IOWA

Collin Brown¹, James Juno¹, Greg Howes¹, Colby Haggerty², Sage Constantinou²
¹ University of Iowa; ² University of Hawaii

Abstract

We analyze a 3D-3V dHybridR, a hybrid particle-in-cell PIC code, simulation of a corrugated non-relativistic quasi-perpendicular magnetized collisionless shock. Quasi-perpendicular shocks with sufficient Mach number have rippling of the shock normal caused by the corrugation instability, which is created by the reflection of ions at the shock. To understand the role this wave has on particle energization, we isolate the ripple as a linear superposition of fields and show that this agrees with linear theory. Our methods enable us to localize instability and plasma mechanisms in space and time. We generate velocity-space signatures using the field-particle correlation technique to look at energy transfer in phase space from just the instability driving the shock ripple. Looking at energy transfer in phase space provides the ability to understand the differing dynamics of distinct populations of particles in phase space. We show how the corrugation instability impacts the distribution of particles in isolation.

Motivations

- Identify instabilities and mechanisms present in collisionless shocks
- Analyze particle energization by instabilities in collisionless shocks using full 3D-3V simulations on a kinetic scale

Introduction

- Shock forms when supersonic flow encounters a stagnate object (ex: Earth's bow shock, Supernova remnants)
- Two dominant parameters: the Alfvén mach speed of the shock, M_A , and the shock normal angle, Θ_{Bn}
- Simulated $M_A = 7.8$ $\Theta_{Bn} = 45^\circ$ shock with dHybridR, a hybrid particle in cell code
- With enough free energy, **shock normal ripples due to corrugation instability(s)**

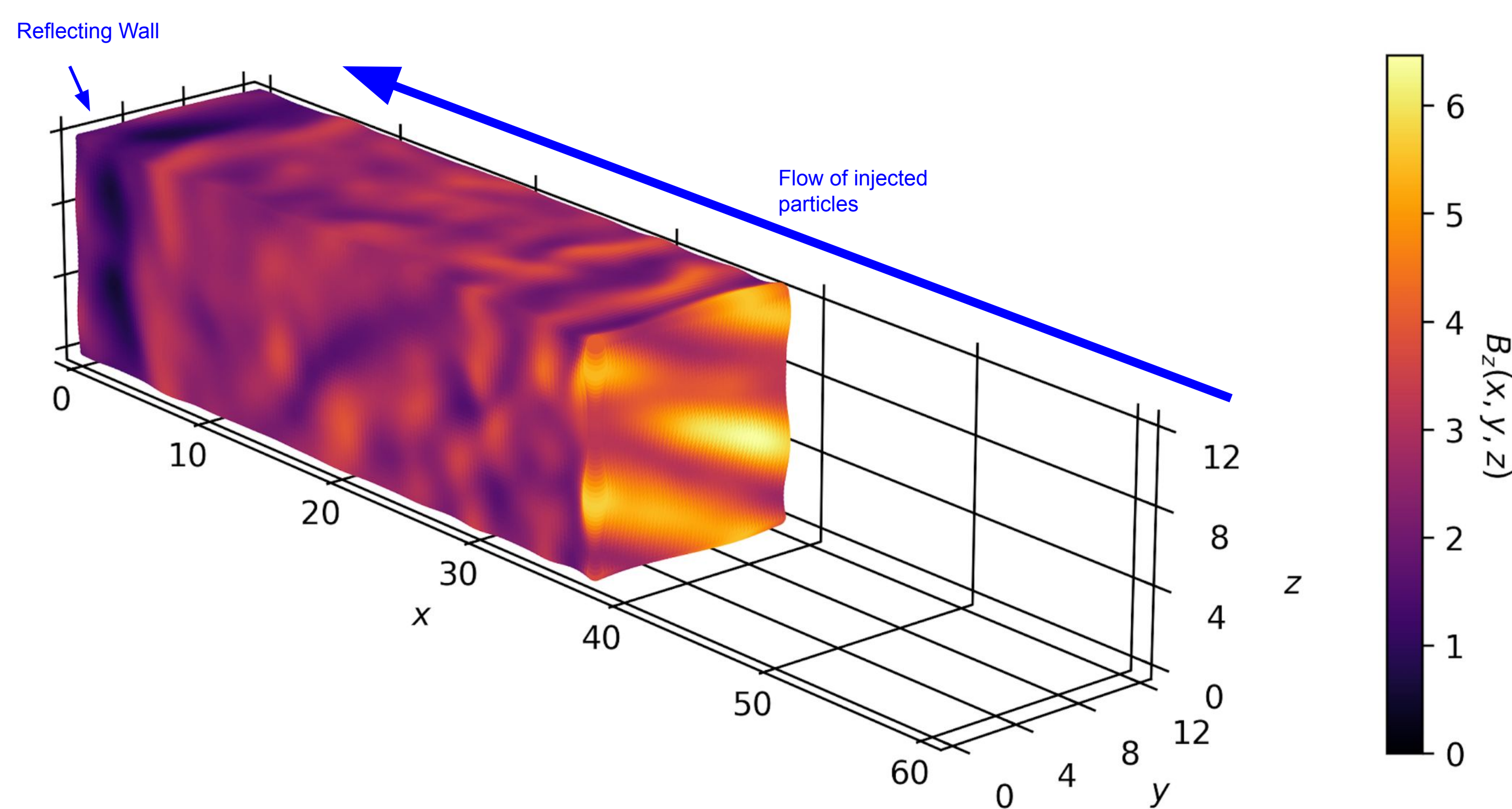
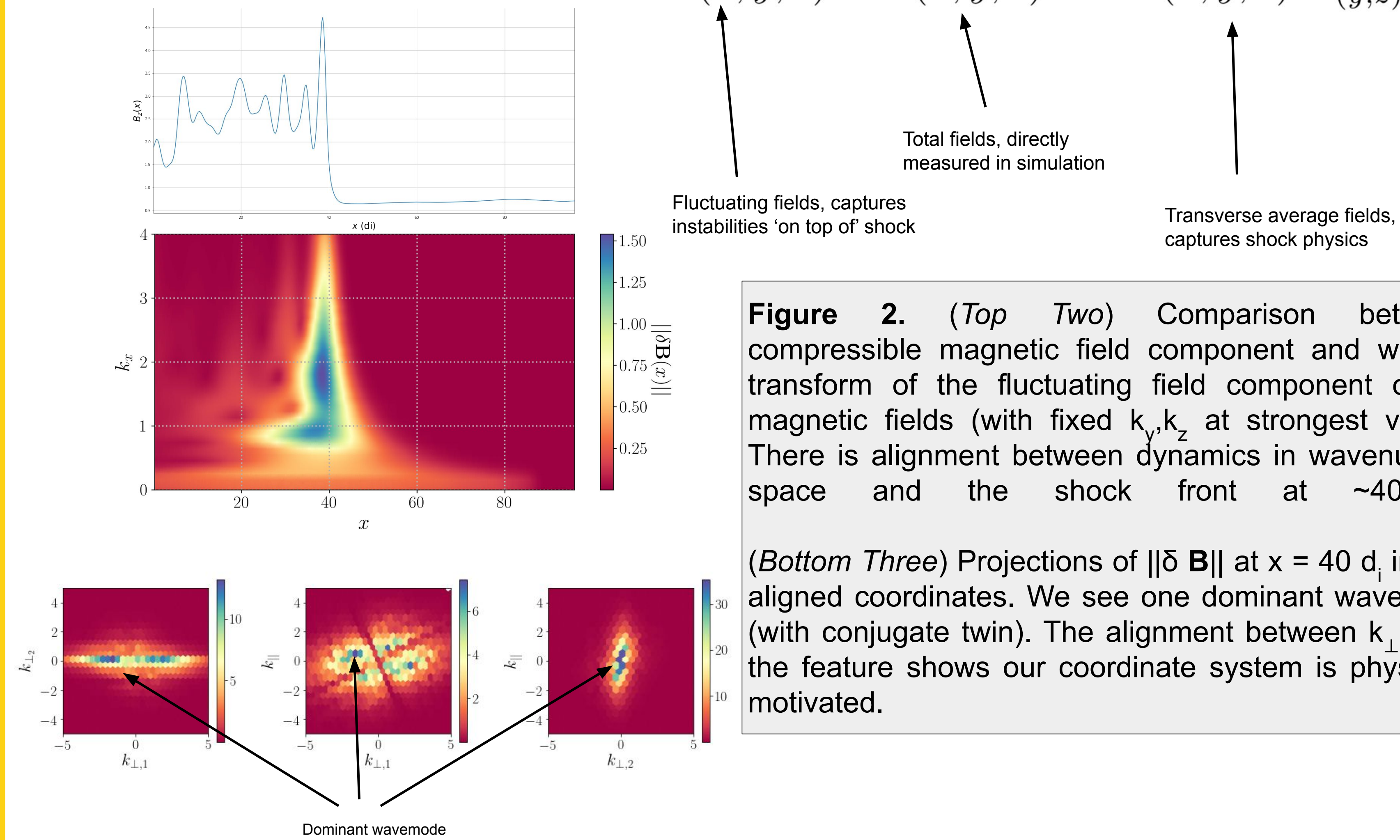


Figure 1. 3D plot of the compressible magnetic field component of a dHybridR simulation of a moderately supercritical quasi-perpendicular shock ($M_A = 7.8$, $\Theta_{Bn} = 45^\circ$). The fields at $x > 38.0 d_i$ are hidden to show the rippling of the shock normal. The shock forms as injected particles reflect off the reflecting wall and interact with the incoming beam.

Instability Isolation



$$\delta \mathbf{E}(x, y, z) = \mathbf{E}(x, y, z) - \langle \mathbf{E}(x, y, z) \rangle_{(y, z)}$$

Fluctuating fields, captures instabilities 'on top of' shock
 Total fields, directly measured in simulation
 Transverse average fields, captures shock physics

Figure 2. (Top Two) Comparison between compressible magnetic field component and wavelet transform of the fluctuating field component of the magnetic fields (with fixed k_y, k_z at strongest value). There is alignment between dynamics in wavenumber space and the shock front at $\sim 40 d_i$.

(Bottom Three) Projections of $\|\delta \mathbf{B}\|$ at $x = 40 d_i$ in field aligned coordinates. We see one dominant wavemode (with conjugate twin). The alignment between $k_{\perp 1, 2}$ and the feature shows our coordinate system is physically motivated.

Instability Identification

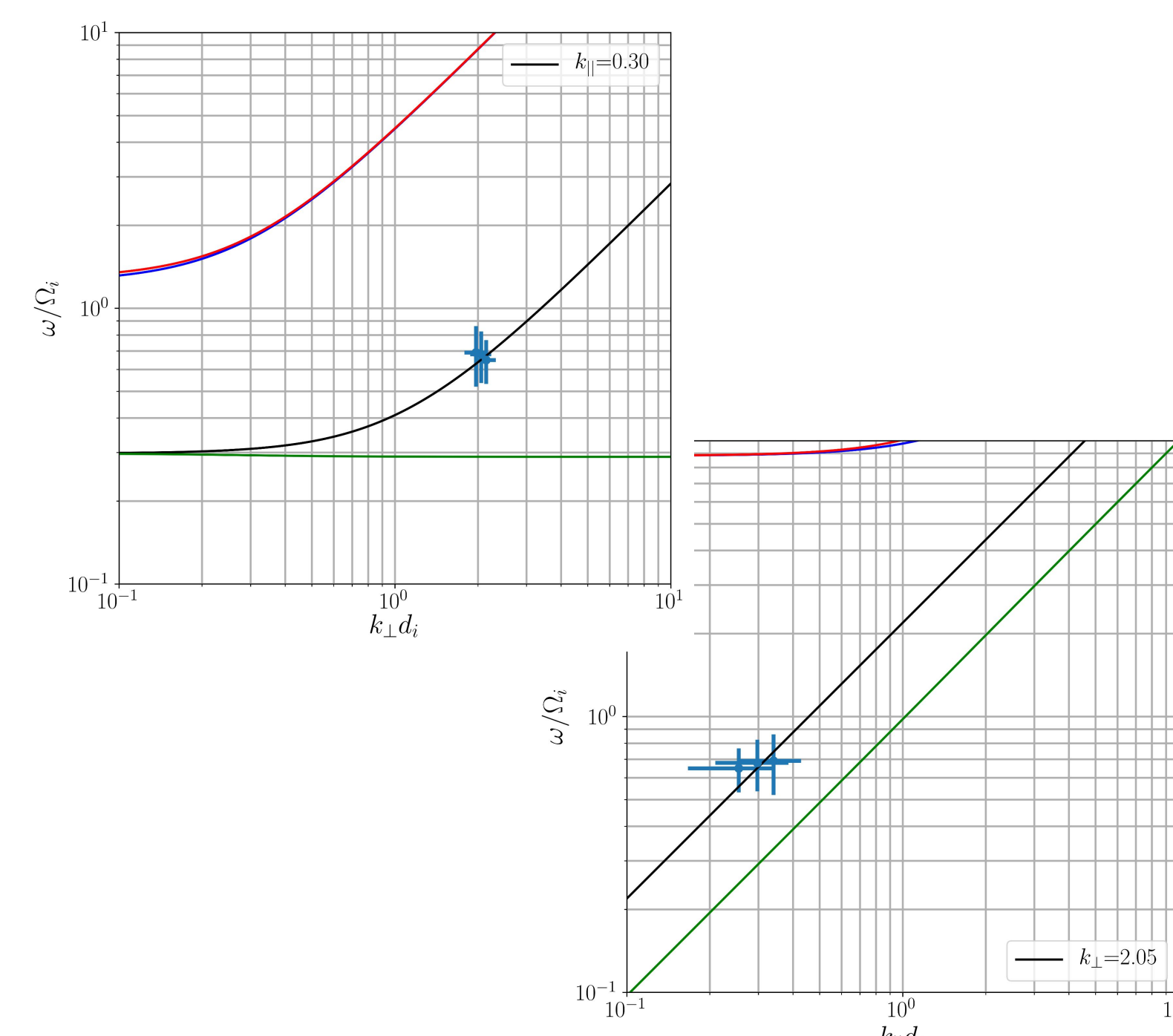


Figure 3. Comparison between three neighboring wave vectors (3 points) with largest Poynting flux (these modes correspond to shock ripple in the ramp) and relevant dispersion relations: Kinetic Alfvén Wave (black), Fast Magnetosonic/Whistler wave for nearly perpendicular propagation (red), and Fast Magnetosonic Wave for any angle of propagation (blue), Slow Magnetosonic Wave (green).

This provides strong evidence that the ripple is Alfvénic and thus the instability present here is the Alfvén Ion Cyclotron instability

Instability Energization throughout the Shock

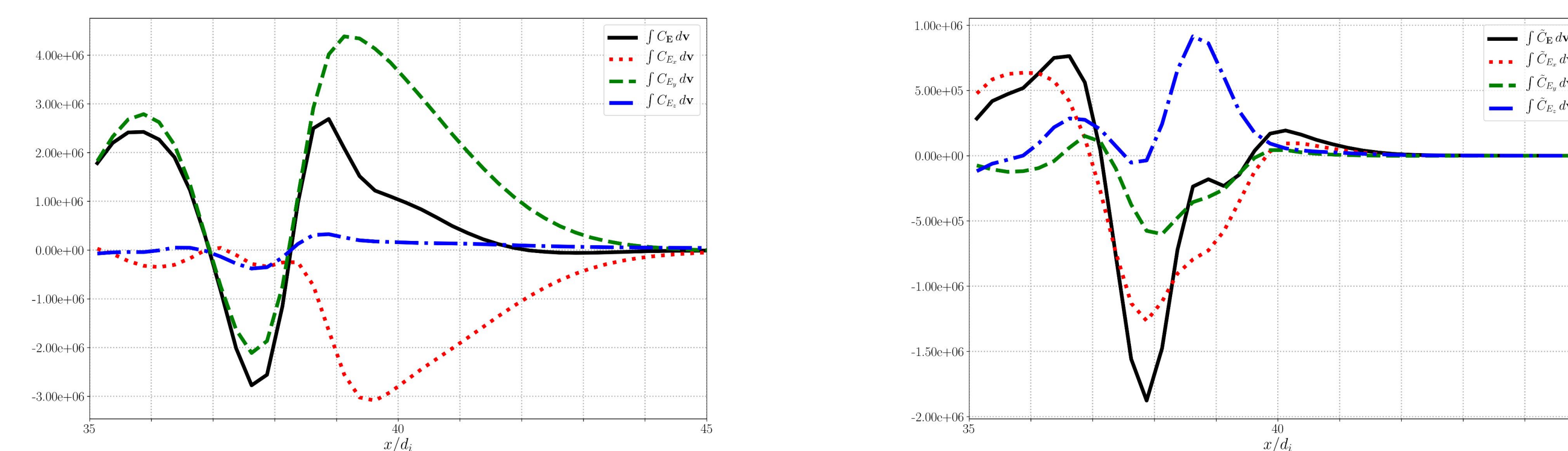


Figure 4. The rate at which the total fields do work on charges in the volume (note that $\mathbf{J} \cdot \mathbf{E} = \int C_E dv$) vs. position in the shock (top) and this rate for fluctuating fields (bottom). We see no transfer of energy in the upstream region, and a net positive transfer of energy in the ramp of the shock ($\sim 40 d_i$). These curves show the complex differences of particle energization in the foot, ramp, and overshoot regions of the shock.

Methodology

Isolating and Identifying Instabilities

- Separate fields into transverse average (captures shock physics) and fluctuating quantities (captures instabilities)
- Use mixture of fourier transform in y and z with **wavelet transform** in x on fluctuating fields to measure "fourier coefficients" locally
 - Find single dominant wavemode (figure 2)
- Use fourier coefficients with Faraday's law in frequency space to measure frequency
 - Compare with linear dispersion relations (figure 3)

Analyzing Particle Energization

- Use the field-particle correlation technique (C_{Ei}) to analyze energization of particles
 - Measures **correlation between fields and change in phase space energy density**
 - Create **velocity-space signatures** (figure 5)
 - Red signatures correspond to an increase in phase-space energy density
 - Use a particular form to maintain locality of fields at each particle (Chen et al 2019)
- Can correlate with just fluctuating fields to measure particle energization due to instability in isolation (\tilde{C}_{Ei})

$$C'_{E_i}(\mathbf{v}) = \left\langle qv_i f(\mathbf{r}, \mathbf{v}, t_0) E_i(\mathbf{r}) \right\rangle_{\mathbf{r}}$$

$$C_{E_i}(\mathbf{v}) = -\frac{v_i}{2} \frac{\partial C'_{E_i}(\mathbf{v})}{\partial v_i} + \frac{C'_{E_i}(\mathbf{v})}{2}$$

$$= \left\langle -q \frac{v_i^2}{2} \frac{\partial f(\mathbf{r}, \mathbf{v}, t_0)}{\partial \mathbf{v}} \cdot E_i(\mathbf{r}) \right\rangle$$

Particle Energization in Velocity Space

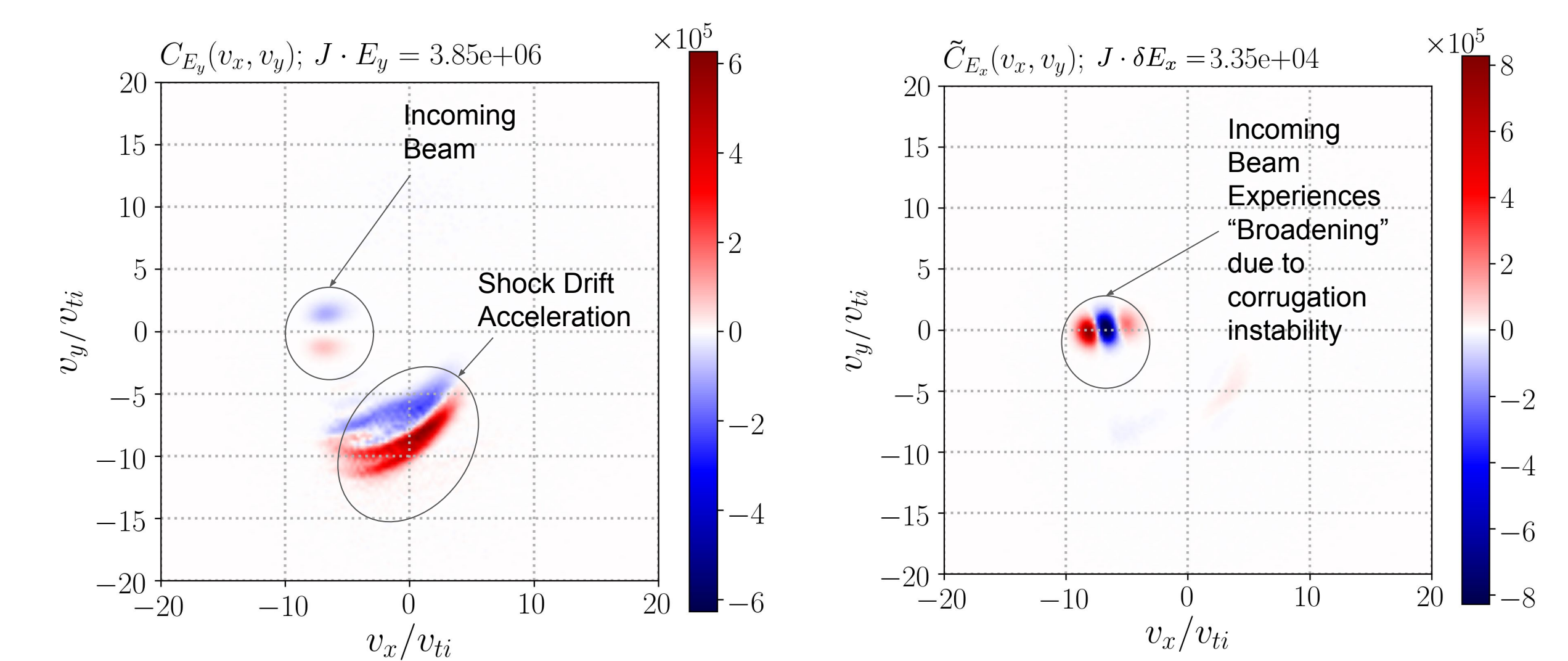


Figure 5. Velocity-space signatures in the ramp that show particle energization in phase space due to the total fields (left) and the fluctuating fields (right). We see that the total fields are responsible for accelerating the reflected particles while the fluctuating fields (i.e. the local shock ripple), has negligible impact on the reflected particles, but contributes a small amount of "broadening" to the incoming beam.

References

Chen, C. H. K., K. G. Klein, and Gregory G. Howes. "Evidence for electron Landau damping in space plasma turbulence." Nature communications 10.1 (2019): 1-8.